J. Microbiol. Biotechnol. (2015), 25(11), 1827–1834
http://dx.doi.org/10.4014/jmb.1506.06079

jmb

The Role of Residues 103, 104, and 278 in the Activity of SMG1 Lipase from *Malassezia globosa*: A Site-Directed Mutagenesis Study

Dongming Lan[1], Qian Wang[2], Grzegorz Maria Popowicz[3], Bo Yang[2], Qingyun Tang[1], and Yonghua Wang[1]*

[1]*College of Light Industry and Food Sciences, South China University of Technology, Guangzhou 510641, P.R. China*
[2]*School of Bioscience and Bioengineering, South China University of Technology, Guangzhou 510006, P.R. China*
[3]*Institute of Structural Biology, Helmholtz Zentrum München, Deutsches Forschungszentrum für Gesundheit und Umwelt (GmbH), D-85764 Neuherberg, Germany*

Received: July 1, 2015
Revised: August 1, 2015
Accepted: August 4, 2015

First published online
August 4, 2015

**Corresponding author*
Phone: +86-20-87113842;
Fax: +86-20-87113842;
E-mail: yonghw@scut.edu.cn

pISSN 1017-7825, eISSN 1738-8872

The SMG1 lipase from *Malassezia globosa* is a newly found mono- and diacylglycerol (DAG) lipase that has a unique lid in the loop conformation that differs from the common alpha-helix lid. In the present study, we characterized the contribution of three residues, L103 and F104 in the lid and F278 in the rim of the binding site groove, on the function of SMG1 lipase. Site-directed mutagenesis was conducted at these sites, and each of the mutants was expressed in the yeast *Pichia pastoris*, purified, and characterized for their activity toward DAG and *p*-nitrophenol (pNP) ester. Compared with wild-type SMG1, F278A retained approximately 78% of its activity toward DAG, but only 11% activity toward pNP octanoate (pNP-C8). L103G increased its activity on pNP-C8 by approximately 2-fold, whereas F104G showed an approximate 40% decrease in pNP-C8 activity, and they both showed decreased activity on the DAG emulsion. The deletion of 103-104 retained approximately 30% of its activity toward the DAG emulsion, with an almost complete loss of pNP-C8 activity. The deletion of 103-104 showed a weaker penetration ability to a soybean phosphocholine monolayer than wild-type SMG1. Based on the modulation of the specificity and activity observed, a pNP-C8 binding model for the ester (pNP-C8, N102, and F278 form a flexible bridge) and a specific lipid-anchoring mechanism for DAG (L103 and F104 serve as "anchors" to the lipid interface) were proposed.

Keywords: Lipase, substrate selectivity, lid, site-directed mutation

Introduction

Lipases (E.C. 3.1.1.3) are a part of the family of hydrolases that act on carboxylic ester bonds. They have been used in many applications, such as flavor synthesis [6], oil/fat modification [16, 17], and biodiesel production [1]. Most of the lipases contain an amphiphilic α-helical motif "lid" covering the active site to prevent the substrate from accessing the catalytic pocket in solution. The lid undergoes conformational rearrangement when a lipase attaches to the oil-water interface, exposing the catalytic site to solvents and making it accessible for the substrate. This mechanism is called "interfacial activation" [22].

Recently, mono- and diacylglycerol (DAG) lipases have attracted attention because of their physiological functions [15] and application for oil and fat modification [23, 25]. In previous studies, mono- and diacylglycerol lipases from *Malassezia globosa* (named Lip1 or SMG1) have been biochemically characterized [7, 23], and crystal structures of SMG1 (PDB entry: 3UUE and 3UUF) have been resolved by our group [26]. The structure reveals that it has a unique lid conformation (lacking a secondary structure), which differs from the typical α-helix conformation previously described [3, 5, 14].

The lid is found to be closely related to lipase substrate selectivity [4, 8, 11, 18]. Substrate selectivity is a determinant factor for lipase application. Most lipases with α-helix lids display almost no activity against their substrates in the

soluble state, but undergo activation when the substrate reaches a micellization concentration. However, some lipases (such as CALB or GPL) with atypical lid conformations do not obey this mechanism, showing activity on substrates at low concentrations [13]. Based on these findings, the substrate recognition mechanism of SMG1 may be different from that of common lipases owing to its unique lid in the loop conformation; however, the evidence of this is limited.

To address this problem, we employed site-directed mutagenesis to create SMG1 variants. Residues around the lid region and active site of SMG1 (Leu 103, Phe 104, and Phe 278) were selected for investigation. The biochemical properties and binding ability to phosphocholine monolayers of the SMG1 mutants were tested. DAG and *p*-nitrophenol (pNP) ester were used as substrates. The modulation of the specificity and activity observed allowed for the construction of the substrate binding model, and the substrate recognizing mechanisms were discussed.

Materials and Methods

Strains, Chemicals, Plasmids, and Medium

Escherichia coli DH5 alpha was used as the cloning host, and plasmid pGAPZαA (Invitrogen, Carlsbad, CA, USA) was used as the cloning vector. The *Pichia pastoris* (*P. pastoris*) X-33 (Invitrogen) strain was used for the expression of recombinant proteins. Soybean phosphatidylcholine (PC), pNP, and pNP octanoate (pNP-C8) were purchased from Sigma-Aldrich. DAG-rich oil (>99%) was prepared in the laboratory as previously described [27]. HPLC-grade *n*-hexane and 2-propanol were purchased from Kermel Chemical Reagent (Tianjing, China). All other chemicals were of analytical grade.

Mutant Construction, Expression, and Purification

The SMG1 gene was cloned into the plasmid pGAPZαA and was fused with a His_6 tag at its C-terminus by using a previously constructed vector as the template [10]. Site-directed mutagenesis of the SMG1 gene was carried out by the overlap extension PCR method. The PCR products were double-digested by *Kpn*I/*Sal*I and cloned into the same site of the pGAPZαA vector. The primers used in this study are listed in Table 1. All of the constructions were confirmed by DNA sequencing and then linearized by restriction enzyme *Bln*I and transformed into the *P. pastoris* X-33 strain by electroporation according to the protocol provided by the manufacturer. Zeocin-resistant clones with the highest expression levels were selected based on time-course experiments by SDS-PAGE analysis.

P. pastoris X-33 cells containing the recombinant plasmids were grown in YPD liquid medium at 30ºC with a shaking speed of 200 rpm for 72 h. The supernatant of the fermentation broth after centrifugation (10,000 ×*g*, 20 min, 4ºC) was filtered through a 0.22 μm filter membrane and then concentrated and buffer-exchanged to buffer A (20 mM sodium phosphate, 0.5 M NaCl, and 30 mM imidazole, pH 7.4, at 4ºC) through a 10 kDa cutoff membrane (Vivaflow 200, Sartorius, Germany). Buffer A, containing the crude enzyme sample, was loaded onto a HisTrap HP column and washed with buffer A again. Then, buffer B (20 mM sodium phosphate, 0.5 M NaCl, and 500 mM imidazole, pH 7.4) was used to wash the target proteins off of the column. The purity of the recombinant lipase in the elution was analyzed by 12% SDS-PAGE. The protein concentrations were determined with the BCA Protein Assay Kit (Sangon Biotech Shanghai Co., Ltd., Shanghai, China).

Activity Determination

The lipase activity on the pNP ester was determined by a colorimetric method using pNP-C8 as a substrate as previously described [12]. The reaction mixture consisted of 80 μl of buffer at the desired pH value, 10 μl of purified enzyme solution at the proper concentration, and 10 μl of 10 mM substrate dissolved in ethanol. The reaction was incubated at the desired temperature for 5 min and terminated by adding 100 μl of a solution containing 1% SDS and 0.1 M Tris. The absorbance of the reaction mixture was measured at 405 nm. One unit of enzyme activity was defined as the amount of enzyme required to release 1 μmol of pNP per minute.

The activity of the lipase was assayed by titration using a DAG-rich oil emulsion (polyvinyl alcohol:DAG; 3:1) as the substrate.

Table 1. Primers used for mutant construction.

Primer name	Sequence
F278A forward	5'-gttgctcgcgagttcaacgctgacgaccaccaaggtatc-3'
F278A reverse	5'-gataccttggtggtcgtcagcgttgaactcgcgagcaac-3'
L103G forward	5'-ccatcgagggcacgaacggtttctcgcttaactcgg-3'
L103G reverse	5'-ccgagttaagcgagaaaccgttcgtgccctcgatgg-3'
F104G forward	5'-catcgagggcacgaacctttgctcgcttaactcg-3'
F104G reverse	5'-cgagttaagcgagccaaggttcgtgccctcgatgg-3'
Delete103-104 forward	5'-gagggvacgaactcgcttaactcgg-3'
Delete103-104 reverse	5'-ccgagttaagcgagttcgtgccctc-3'

The assay medium, which consisted of 2.5 ml of the oil emulsion and 2 ml of phosphate buffer (0.1 M, pH 6), was incubated at 25°C for 10 min. Then, 0.5 ml of enzyme was added, and the mixture was incubated for 10 min at 25°C with an agitation rate of 150 rpm. The reaction was terminated by the addition of 10 ml of ethanol, and titration was carried out with 0.05 M NaOH. For comparison, a heat-inactivated lipase enzyme was used as a control. One unit of enzyme activity was defined as μmoles of free fatty acids released per milliliter per minute under the assay conditions. All of the results are presented as the mean of duplicate measurements.

Optimum pH and Temperature Assay

The optimum pH for the purified lipase activity was determined at 25ºC using pNP-C8 as a substrate. Buffers with pH values ranging from 4.0 to 8.0 (pH 4.0–5.0: 0.1 M sodium citrate-0.1 M citric acid; pH 6.0–7.0: 0.1 M phosphate buffer; pH 8: 0.05 M Tris-HCl) were used. The optimum temperature of the lipase activity was determined at pH 6.0. The temperature was set from 10°C to 40°C.

Kinetic Analysis

The specific activities of wild-type (Wt) and mutant SMG1 against pNP-C8 were determined at nine different substrate concentrations over the concentration range 0.02–1 mM at the optimal pH and temperature. The kinetic constants (k_{cat}, K_m, and k_{cat}/K_m) were calculated by fitting the initial rate data into the Michaelis-Menten equation in GraphPad Prism 6.

Lipase Adsorption onto Soybean-PC Monomolecular Films

Lipase adsorption-induced surface pressure changes on the lipid monolayer were recorded with the Microtrough X (Kibron Inc., Espoo, Finland). The cylindrical trough was filled with 0.1 M phosphate buffer (pH 6.0), and the monomolecular film was prepared by spreading various volumes of soybean-PC solution in chloroform (1 mg/ml). After the initial surface pressure (π_i) of monomolecular films had stabilized, SMG1 lipase or its mutants (0.088 μM, final concentration) was injected into the aqueous subphase. A magnetic bar was continuously stirred with a rotating speed of 168 ×*g* to homogenize the aqueous phase. The surface pressure increase due to the adsorption of enzymes to the film was continuously recorded until the equilibrium surface pressure was reached. The critical surface pressure (π_c) of the lipases tested was determined according to the method described by Ben Salah *et al*. [2].

Model of pNP-C8 in the Binding Pocket of SMG1

The three-dimensional coordinates of the pNP-C8 model and the dictionary were generated with the PRODRG program [19]. The position and conformation of pNP-C8 were handled by Coot using rotation and Chi angle editing tools [9]. The conformation of pNP-C8 was optimized by energy minimization.

Results and Discussion

Mutagenesis Sites Selection

The lipase lid has been reported to play an important role in interface adsorption, substrate selectivity, and thermostability [20, 21]. The crystal structure of SMG1 showed a unique lid in the loop conformation instead of the helix, as seen in common lipases, such as RML (lipase from *Rhizomucor miehei*) and HLL (lipase from *Humicola lanuginosa*) (Fig. 1). In the structure of SMG1, residues Asn102 (located at the N-terminus of the lid) and Phe278 (located at the rim of the binding site groove over the catalytic His281) formed a bridge-like structure covering catalytic Ser171 and His281 (Fig. 2A). Residues Leu103 and Phe104 are adjacent to Asn102, are located at the surface of SMG1, and are not buried as deeply as other residues in the lid region. The catalytic site of SMG1 was not completely obstructed by the lid. Therefore, the closed lid conformation may still allow smaller substrates (such as the pNP ester, with a short acyl chain length) to enter and undergo hydrolysis, whereas lid-opening is necessary to process

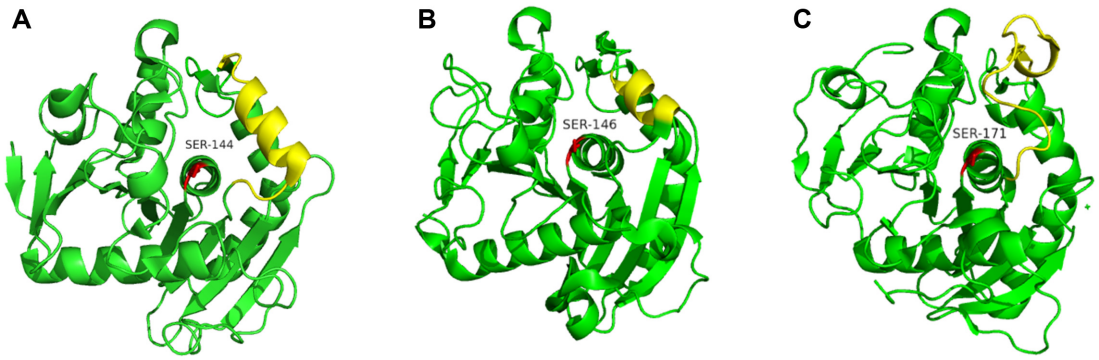

Fig. 1. Structure of RML (**A**, PDB entry: 4TGL), HLL (**B**, PDB entry: 1DTE) and SMG1 lipase (**C**, PDB entry: 3UUE). The active site of each lipase is shown as a red stick. The lid domain of each lipase is marked in yellow.

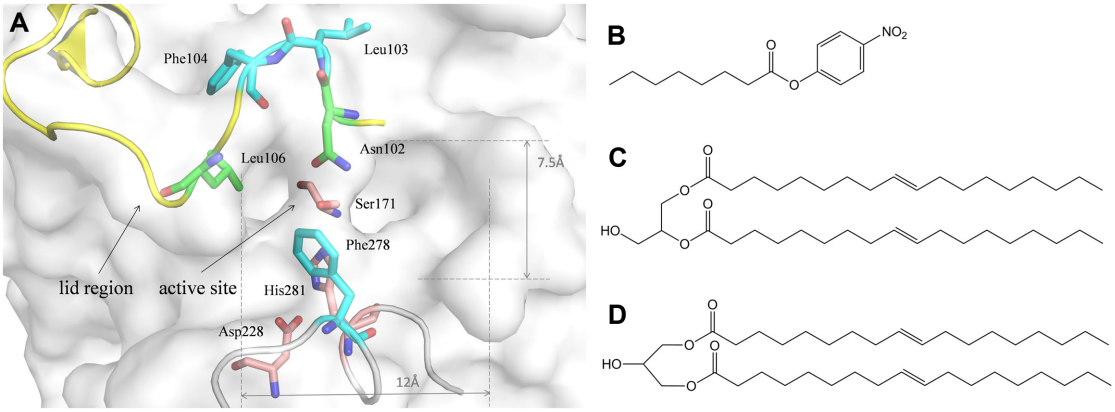

Fig. 2. Binding pocket and lid region of SMG1 (PDB entry: 3UUE) in a surface representation as well as the chemical formulas of the substrates used in the study.

(**A**) The lid region is shown as a cartoon and colored yellow. The mutated sites and the catalytic triad are colored in cyan and pink, respectively. (**B**) pNP-C8. (**C**) 1,2-Dioleoly glycerol. (**D**) 1,3-Dioleoly glycerol.

DAG (Fig. 2A) or other larger substrates. Furthermore, Leu103 and Phe104, hydrophobic amino acids harboring bulky side chains, may contribute to the catalytic performance of SMG1 by affecting the binding capability to the hydrophobic interface. To confirm this assumption, seven SMG1 variants, namely L103G, F104G, F278A, L103G-F278A, F104G-F278A, Delete103-104, and F278A-Delete(103-104), were constructed.

Biochemical Properties of the Mutants

SMG1-Wt and mutants were expressed in *P. pastoris* and were purified by metal-chelating chromatography to a single band (data not shown). The optimal pH, optimal temperature, and kinetic constants were determined using pNP-C8 as a substrate. As seen from Table 2, most of the mutants had the same optimal pH as SMG1-Wt, and only the F104G and Delete103-104 mutants had a minor drop in optimal pH from 6 to 5. L103G, F278A, and F104G-F278A showed a decreased optimal temperature, from 25°C to 15°C, and F104G showed a decreased optimal temperature, from 25°C to 20°C, whereas L103G-F278A and Delete103-104 showed an increased optimal temperature to 35°C and 30°C, respectively. To investigate whether the mutagenesis affected the catalytic efficiency of SMG1, the kinetic constants of SMG1 and its mutants were determined. L103G showed an increase of 3.8-fold in the k_{cat}/K_m value compared with that of SMG1-Wt, whereas the kinetic constants for the other mutants decreased or remained at the same level as that of SMG1-Wt. The activity of F278A-Delete(103-104) was too low to reliably calculate the enzymatic constants.

Phe278 Is a Major SMG1 Specificity Determinant

For catalyzing the pNP-C8 ester, Phe278 is a major SMG1 specificity determinant. The F278A mutation had a large impact on the processing of an aromatic pNP-C8 ester (11% of the activity was retained in the F278A mutant, Fig. 3), whereas its influence on DAG processing was negligible (78% retained). The Phe278 residue is located at the rim of the binding site groove over catalytic His281 (Fig. 2A). Its

Table 2. Optimal pH, temperature, and kinetic constants of SMG1 and its mutants.

	Optimal pH	Optimal T (°C)	k_{cat} (s^{-1})	K_m (mM)	k_{cat}/K_m (mM/s)
SMG1-Wt	6	25	23.45 ± 2.57	0.59 ± 0.13	39.59
L103G	6	15	54.03 ± 3.26	0.35 ± 0.05	152.3
F104G	5	20	18.77 ± 1.78	0.37 ± 0.09	50.22
F278A	6	15	2.11 ± 0.07	0.71 ± 0.05	2.97
L103G-F278A	6	35	1.16 ± 0.10	0.20 ± 0.05	5.82
F104G-F278A	6	15	4.10 ± 0.41	0.79 ± 0.15	5.21
Delete103-104	5	30	0.33 ± 0.12	1.38 ± 0.75	0.23

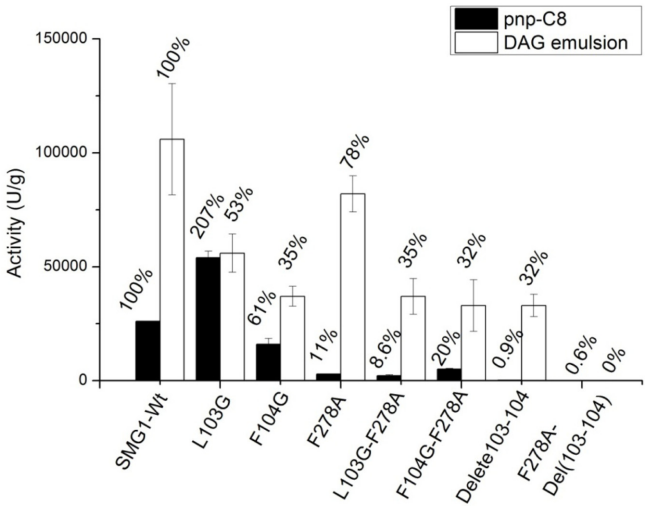

Fig. 3. Hydrolysis activities of SMG1 mutants toward pNP-C8 and DAG.

The hydrolysis activity of SMG1-Wt toward pNP-C8 or DAG was set to 100%. All of the other values were standardized to this reference value.

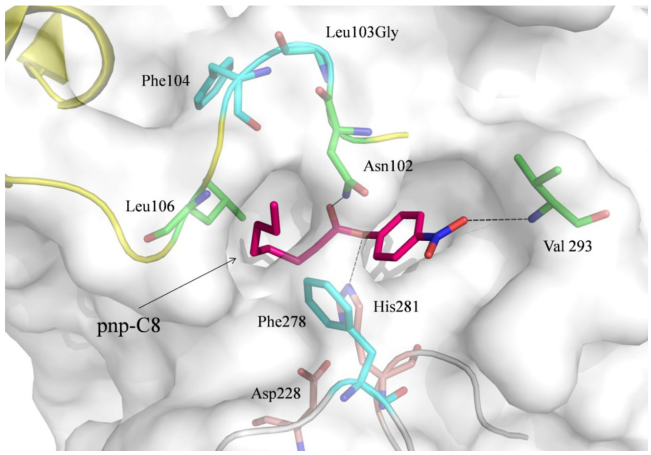

Fig. 4. Model of pNP-C8 in the active site of SMG1-L103G.

The substrate of SMG1, pNP-C8, is shown as a stick and colored hot pink. The residues involved in the catalytic sites and binding model are labeled. The hydrogen bonds from pNP-C8 to the residues are shown as black dashes. The substrate aromatic ring is at an optimal distance for aromatic stacking with the Phe278 ring.

bulky side chain divides the binding groove directly over the enzyme active site. An analysis of the electron density data from previous structural studies indicates that the aromatic ring of Phe278 is able to flip into different conformations, thus allowing adaptation to different ligands. Notably, the natural DAG substrate is minimally affected by the F278A mutation, but the aromatic pNP-C8 ester is processed much slower. This indicates that the presence of aromatic stacking between Phe278 and the aromatic substrate stabilized it in the active site in enzymatically optimal configurations. Purely aliphatic DAG is minimally affected owing to a lack of aromatic stacking. The minor drop in F278A activity toward DAG can be attributed to the worse stabilization of the substrate by the wider binding groove.

Leu103 and Phe104 Are Involved in Interfacial Adsorption

To investigate the lid fragment function in catalytic selectivity, DAG and pNP esters were selected as substrates to test enzyme activities. It was observed that the L103G mutant showed doubled activity against the pNP-C8 ester (207%; Fig. 3), whereas DAG activity was halved (53%). Because the Leu103 orientation is likely to affect the preceding Asn102, we reasoned that the interaction is formed between a small substrate ester group (pNP-C8) and the carboxamide of Asn102, which helps to orient the ligand in the active site. The L103G mutation caused a beneficial shift of Asn102, thus improving this phenomenon (Fig. 4). For a larger substrate, such as DAG, this interaction is not necessary or even has a negative effect, as other hydrophobic interactions take part in its stabilization. Surprisingly, we did not observe a similar phenomenon for the F104G mutant, which is thought to be more relevant for lid mobility. Therefore, we reasoned that the L103G mutation has no direct effect on the lid opening that would allow the entry of the pNP-C8 ester, indicating that a closed SMG1 lid does not prevent the entry of the single aliphatic chain of the ester to the active site. In contrast, branched DAGs require lid opening upon interface activation to enter the active site. The F104G mutation will most likely have an opposite effect on the orientation of Asn102 compared with the L103G mutation. Indeed, for the F104G mutation, and we observed an almost 40% reduction in ester activity. Moreover, both separate Phe278 and Phe104 mutations strongly impaired enzyme processing (with F278A retaining 11% activity and F104G retaining 61% activity toward pNP-C8, respectively, Fig. 3). The double F104G-F278A mutant partially (2-fold) rescued that activity (20% for F104G-F278A) compared with the single F278A mutation (11% for F278A). This result indicates that the substrate binding pose was rearranged in the double mutant in proximity to Phe278 in such a way that the activity was partially restored. Most likely, F104G mutants allow partial lid flexibility and entry of the pNP-C8 aliphatic chain into the hydrophobic groove, which stabilizes it in the catalytically optimal configuration. Thus,

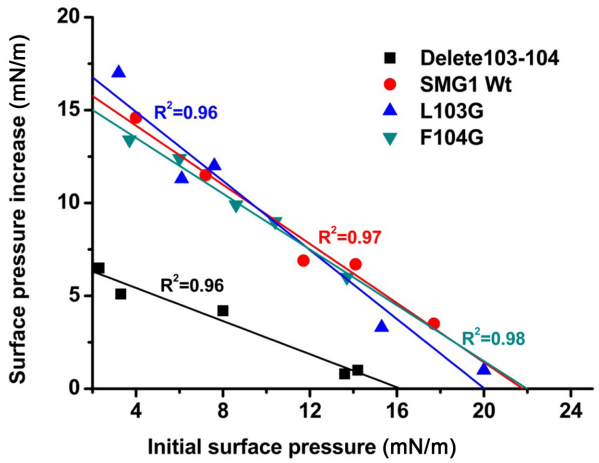

Fig. 5. Interaction of SMG1 and its mutants with soybean-PC monolayers.

The π_i of the monomolecular film ranged from 2 to 20 mN.m^{-1}. After injection of the lipase (3.3 μg) under the soybean-PC monomolecular films, the increase in surface pressure was recorded. The increase in surface pressure was plotted as a function of π_i. The π_c value of the penetration of the SMG1 lipase or its mutants was estimated by linear extrapolation to the zero surface pressure increase of the experimental points. SMG1, L103G, F104G, and Delete103-104 are shown as red, blue, dark cyan, and black lines, respectively. The least square values of each line are indicated.

the detrimental F278A mutation effect is partially rescued. Phe278 and F104G are far apart from each other. In such a case, the influence of both mutations should be uncoupled and the double mutant would have further decreased activity. This observation is further confirmed by the double-deletion mutant Leu103 and Phe104. We observed a complete loss of activity toward the pNP-C8 ester, whereas activity toward DAG remained at a level comparable to the Leu103 and Phe104 point mutations. Thus, it could be presumed that Leu103 and Phe104 may be involved in the interfacial adsorption.

To prove the above assumption, the capacity of interfacial adsorption for SMG1 and its mutants were studied by the monolayer technique. Soybean-PC was used to generate a monomolecular film because SMG1 and its mutants could not hydrolyze PC [24]. The surface pressure will increase when lipases penetrate into the PC monolayer. π_c has been considered to be an indicator of the capacity of a protein to penetrate into a monomolecular film. It can be determined by linear extrapolation to a zero surface pressure increase. As shown in Fig. 5, similar π_c values of approximately 22 mN/m were observed for F104G and SMG1-Wt. L103G showed a slightly decreased π_c of approximately 20 mN/m, whereas the double deletion of L103 and F104 resulted in a significant decrease of π_c (approximately 16 mN/m). This indicated that the penetration capacity of the Delete103-104 mutant into a monomolecular film was weaker than that of SMG1-Wt. This result is in agreement with the lower specific activity of Delete103-104 toward the DAG substrate compared with that of SMG1-Wt, suggesting that L103 and F104 are involved in the interfacial adsorption.

The Lid Region of SMG1 Lipase Using a Specific Lipid-Anchoring Mechanism

The structural analysis of the SMG1 substrate binding site indicated that its active center was not covered by the α-helix, as seen in other lipases [3, 5] (Fig. 1). The active site was only covered by an Asn102/Phe278 bridge that is partially flexible. The open part of the substrate groove spanned approximately 12 Å in length and 7.5 Å in width (Fig. 2A). The lid region blocked the more distant part of the groove, with Leu106 being the first residue limiting its size. The lid is expected to open upon contact with the lipase in a lipophilic environment. Therefore, its activity is restrained in the aqueous phase. We mutated Leu103 and Phe104 to Gly to investigate their influence on the lid behavior and substrate specificity. The influence of the L103G mutation for SMG1 function in the aqueous phase has been described in a previous section. Both mutations reduced the lipophilic character of the lid beginning and, as expected, reduced the enzymatic activity against micelle-forming DAG. The mutations reduced the overall enzyme activity for DAG (53% for L103G and 35% for F104G; Fig. 3). The increased activity of the L103G mutant on the ester substrate was explained in a previous section. For F104G, we observed half of the Wt activity against the ester (61%). The mutations were expected to "open" the lid and improve enzymatic activity toward larger substrates, such as DAG; however, we observed an opposite effect. Because the opening of the lid is necessary for the lipid substrate to enter into the binding groove, it is evident that both Leu103 and Phe104 serve as "anchors" for the enzyme entering the lipophilic phase. Their elimination, while improving lid flexibility, leads to decreases in enzymatic activity against DAG. From our experiment, we reasoned that both Leu103 and Phe104 helped to attach the enzyme and "open" the lid in a lipophilic environment. This mechanism is further confirmed by the fact that the double deletion of both residues (deletion of Leu103 and Phe104) did not lead to a significant change in DAG activity versus the point mutations. Therefore, in all cases, the loss of activity for

DAG was caused by impaired lipid-phase entry rather than binding site obstruction.

In conclusion, structure-guided protein engineering is an effective strategy to develop biocatalysts for industrial application. The crystal structure of the SMG1 lipase was previously resolved by our group, and Leu103, Phe104, and Phe278 may be involved in affecting the catalytic activity of SMG1 lipase according to structural analysis. Biochemical characterization and interfacial adsorption analysis have demonstrated that this supposition was correct. Our work may shed some light on the molecular basis of lipase structure-function relationships.

Acknowledgments

This work was made possible with funding provided by the National Science Funds for the Excellent Youth Scholars (No. 31222043), the National Natural Science Foundation of China (21406076), the PhD Start-up Fund of Natural Science Foundation of Guangdong Province of China (2015A030310381) (No. 2015ZM059).

References

1. Akoh CC, Chang SW, Lee GC, Shaw JF. 2007. Enzymatic approach to biodiesel production. *J. Agric. Food Chem.* **55:** 8995-9005.
2. Ben Salah A, Sayari A, Verger R, Gargouri Y. 2001. Kinetic studies of *Rhizopus oryzae* lipase using monomolecular film technique. *Biochimie* **83:** 463-469.
3. Brady L, Brzozowski AM, Derewenda ZS, Dodson E, Dodson G, Tolley S, *et al.* 1990. A serine protease triad forms the catalytic centre of a triacylglycerol lipase. *Nature* **343:** 767-770.
4. Brocca S, Secundo F, Ossola M, Alberghina L, Carrea G, Lotti M. 2003. Sequence of the lid affects activity and specificity of *Candida rugosa* lipase isoenzymes. *Protein Sci.* **12:** 2312-2319.
5. Brzozowski AM, Savage H, Verma CS, Turkenburg JP, Lawson DM, Svendsen A, Patkar S. 2000. Structural origins of the interfacial activation in *Thermomyces (Humicola) lanuginosa* lipase. *Biochemistry (Mosc.)* **39:** 15071-15082.
6. Cao M, Fonseca LM, Schoenfuss TC, Rankin SA. 2014. Homogenization and lipase treatment of milk and resulting methyl ketone generation in blue cheese. *J. Agric. Food Chem.* **62:** 5726-5733.
7. DeAngelis YM, Saunders CW, Johnstone KR, Reeder NL, Coleman CG, Kaczvinsky JR, *et al.* 2007. Isolation and expression of a *Malassezia globosa* lipase gene, LIP1. *J. Invest. Dermatol.* **127:** 2138-2146.
8. Dugi KA, Dichek HL, Santamarina-Fojo S. 1995. Human hepatic and lipoprotein lipase: the loop covering the catalytic site mediates lipase substrate specificity. *J. Biol. Chem.* **270:** 25396-25401.
9. Emsley P, Lohkamp B, Scott WG, Cowtan K. 2010. Features and development of Coot. *Acta Crystallogr. D* **66:** 486-501.
10. Gao CL, Lan DM, Liu L, Zhang HJ, Yang B, Wang YH. 2014. Site-directed mutagenesis studies of the aromatic residues at the active site of a lipase from *Malassezia globosa*. *Biochimie* **102:** 29-36.
11. Holmquist M, Martinelle M, Clausen IG, Patkar S, Svendsen A, Hult K. 1994. Trp89 in the lid of *Humicola lanuginosa* lipase is important for efficient hydrolysis of tributyrin. *Lipids* **29:** 599-603.
12. Lan D, Popowicz GM, Pavlidis IV, Zhou P, Bornscheuer UT, Wang Y. 2015. Conversion of a mono- and diacylglycerol lipase into a triacylglycerol lipase by protein engineering. *ChemBioChem* **16:** 1431-1434.
13. Martinelle M, Holmquist M, Hult K. 1995. On the interfacial activation of *Candida antarctica* lipase A and B as compared with *Humicola lanuginosa* lipase. *Biochim. Biophys. Acta* **1258:** 272-276.
14. Noble ME, Cleasby A, Johnson LN, Egmond MR, Frenken LG. 1993. The crystal structure of triacylglycerol lipase from *Pseudomonas glumae* reveals a partially redundant catalytic aspartate. *FEBS Lett.* **331:** 123-128.
15. Nomura DK, Long JZ, Niessen S, Hoover HS, Ng SW, Cravatt BF. 2010. Monoacylglycerol lipase regulates a fatty acid network that promotes cancer pathogenesis. *Cell* **140:** 49-61.
16. Pan XX, Xu L, Zhang Y, Xiao X, Wang XF, Liu Y, *et al.* 2012. Efficient display of active *Geotrichum* sp. lipase on *Pichia pastoris* cell wall and its application as a whole-cell biocatalyst to enrich EPA and DHA in fish oil. *J. Agric. Food Chem.* **60:** 9673-9679.
17. Qin XL, Yang B, Huang HH, Wang YH. 2012. Lipase-catalyzed incorporation of different fatty acids into tripalmitin-enriched triacylglycerols: effect of reaction parameters. *J. Agric. Food Chem.* **60:** 2377-2384.
18. Santarossa G, Lafranconi PG, Alquati C, DeGioia L, Alberghina L, Fantucci P, Lotti M. 2005. Mutations in the "lid" region affect chain length specificity and thermostability of a *Pseudomonas fragi* lipase. *FEBS Lett.* **579:** 2383-2386.
19. Schuttelkopf AW, van Aalten DMF. 2004. PRODRG: a tool for high-throughput crystallography of protein-ligand complexes. *Acta Crystallogr. D* **60:** 1355-1363.
20. Shih TW, Pan TM. 2011. Substitution of Asp189 residue alters the activity and thermostability of *Geobacillus* sp. NTU 03 lipase. *Biotechnol. Lett.* **33:** 1841-1846.
21. Tang L, Su M, Zhu L, Chi L, Zhang J, Zhou Q. 2013. Substitution of Val72 residue alters the enantioselectivity and activity of *Penicillium expansum* lipase. *World J. Microbiol. Biotechnol.* **29:** 145-151.
22. Verger R. 1997. 'Interfacial activation' of lipases: facts and

artifacts. *Trends Biotechnol.* **15:** 32-38.
23. Wang WF, Li T, Qin XL, Ning ZX, Yang B, Wang YH. 2012. Production of lipase SMG1 and its application in synthesizing diacylglyecrol. *J. Mol. Catal. B Enzym.* **77:** 87-91.
24. Wang XP, Xu H, Lan DM, Yang B, Wang YH. 2015. Hydrolysis of lysophosphatidylcholines by a lipase from *Malassezia globosa*. *Eur. J. Lipid Sci. Technol.* DOI: 10.1002/ejlt.201400643.
25. Xu D, Sun LJ, Chen HY, Lan DM, Wang YH, Yang B. 2012. Enzymatic synthesis of diacylglycerols enriched with conjugated linoleic acid by a novel lipase from *Malassezia globosa*. *J. Am. Oil Chem. Soc.* **89:** 1259-1266.
26. Xu TT, Liu L, Hou SL, Xu JX, Yang B, Wang YH, Liu JS. 2012. Crystal structure of a mono- and diacylglycerol lipase from *Malassezia globosa* reveals a novel lid conformation and insights into the substrate specificity. *J. Struct. Biol.* **178:** 363-369.
27. Yuan D, Lan D, Xin R, Yang B, Wang Y. 2014. Biochemical properties of a new cold-active mono- and diacylglycerol lipase from marine member *Janibacter* sp. strain HTCC2649. *Int. J. Mol. Sci.* **15:** 10554-10566.